J. Meas. Sci. Instrum., 2025, 16(4): 578-587.
DOI: 10.62756/jmsi.1674-8042.2025056
http://jmsi.publish.founderss.cn
jmsi@nuc.edu.cn

UAV trajectory planning based on improved bidirectional RRT algorithm

WANG Mengqiao, LIU Erlin*

School of Mechanical Engineering, Lanzhou Jiaotong University, Lanzhou 730070, China

***Corresponding author:** LIU Erlin (liuel@mail.lzjtu.cn)

Received: July 5, 2024 **Revised:** September 3, 2024 **Accepted:** November 8, 2024

Abstract: In response to the problems of low sampling efficiency, strong randomness of sampling points, and the tortuous shape of the planned path in the traditional rapidly-exploring random tree (RRT) algorithm and bidirectional RRT algorithm used for unmanned aerial vehicle (UAV) path planning in complex environments, an improved bidirectional RRT algorithm was proposed. The algorithm firstly adopted a goal-oriented strategy to guide the sampling points towards the target point, and then the artificial potential field acted on the random tree nodes to avoid collision with obstacles and reduced the length of the search path, and the random tree node growth also combined the UAV's own flight constraints, and by combining the triangulation method to remove the redundant node strategy and the third-order B-spline curve for the smoothing of the trajectory, the planned path was better. The planned paths were more optimized. Finally, the simulation experiments in complex and dynamic environments showed that the algorithm effectively improved the speed of trajectory planning and shortened the length of the trajectory, and could generate a safe, smooth and fast trajectory in complex environments, which could be applied to online trajectory planning.

Key words: complex environment; bidirectional RRT algorithm; target orientation strategy; artificial potential field method; triangular inequality cut; cubic B-spline; online trajectory planning

0 Introduction

Along with the progress and development of science and technology, UAVs are widely used in civil[1] and military[2] by virtue of their own excellent performance, and trajectory planning plays a huge role in whether UAVs can take off smoothly and complete the tasks autonomously according to the requirements. Trajectory planning not only requires the UAV to avoid obstacles in the path, but also requires it to reach the target point efficiently and find a stable and safe trajectory. Currently, the main research algorithms include particle swarm algorithm[3], ant colony algorithm[4], A* algorithm, and artificial potential field (APF) method[5,6]. The above algorithms can plan paths in simple maps, but there are problems of high computational complexity and easy to fall into local minima. The RRT algorithm was first proposed as an algorithm that can be used to solve the trajectory planning problem in multidimensional space. The RRT algorithm has few parameters, strong search capability, applicable to path planning problems in various complex environments, and can quickly generate local optimal solutions, but the RRT algorithm has fewer parameters, stronger search capability, and can quickly generate local optimal solutions. The RRT algorithm has strong randomness in sampling points, which leads to blind expansion of the random tree and reduces the planning speed of the algorithm, and the quality of the output path of the algorithm is poor due to the expansion of the node process does not take into account the generation value of the path. With the increasing complexity of the flight environment and the continuous improvement of the trajectory requirements, the improvement of the basic algorithm can not be delayed in order to make the UAV fly more efficiently in complex environments[7,8].

Liu et al. proposed an improved fast search randomized tree algorithm with target bias strategy, which improved the speed but had the problem of low efficiency of the algorithm in complex and narrow environments[9]. Zhang et al. proposed RRT-connect algorithm on the basis of RRT algorithm, which improved the original one-way random numbers into two-way random numbers, greatly improving the efficiency of the search[10]. Yu et al. proposed the RRT* algorithm with the aim of pairwise reselection of parent nodes and rewiring process, which ensured the asymptotic optimality of the algorithm[11]. Hao et al. introduced the artificial potential field method into the RRT algorithm to

improve the smoothness and planning speed of the algorithm's planning path[12]. Liao et al. proposed the use of triangular inequality method to improve the algorithm so that the length of the planned path was reduced and the time is close to the optimum[13]. Zhang et al. used cubic B-spline curves to smooth the searched paths after the generation of global paths generated by the algorithm to ensure the feasibility of the paths[14].

As mentioned above, for the traditional RRT algorithm, scholars have made improvements from multiple perspectives. However, when dealing with more complex environments, there are still issues such as excessive randomness in expansion, uneven and unsmooth trajectories, and insufficient consideration of dynamic environments. In this paper, an improved two-way RRT algorithm was proposed for complex and dynamic environments under the effect of artificial potential field, and a goal-oriented strategy was added to the random sampling. The node growth was affected by the combined force of the obstacle repulsion and the target gravitational force, and the node expansion process took into account the flight performance constraints of the UAV, and the efficiency of trajectory planning was greatly improved by the triangular delimitation method of cropping and the three-time B-spline curve smoothing process. The UAV was able to avoid dynamic obstacles effectively. Finally, simulations in different complex environments verified the effectiveness and superiority of the improved algorithm.

The improvements and innovations for UAV trajectory planning and RRT algorithms are as follows: 1) goal-oriented strategies; 2) combination of artificial potential field and bidirectional RRT; 3) triangular inequality cropping; 4) triple B-spline smoothing; 5) online trajectory planning when dealing with dynamic obstacles; 6) comparison of dynamic algorithms.

1 Analysis of trajectory planning issues

1.1 UAV performance constraints

In addition to the flight environment constraints, UAVs also need to satisfy the kinematic and dynamic constraints of the UAV itself during flight. Under the premise of following a series of constraints, the core task of UAV trajectory planning is to determine an optimal path that satisfies the conditions.

1.1.1 Minimum track segment constraints

Typically, the minimum trajectory segment constraint in UAV trajectory planning refers to the shortest distance to be flown in a straight line before the UAV flight attitude changes. It is usually determined based on factors such as specific mission requirements, UAV size, and flight control capabilities.

In a complex flight environment, UAVs need a certain straight flight distance to adjust their flight status. The shortest flight segment of the trajectory is denoted by $L_{\min}$, then the minimum trajectory segment constraint can be expressed as

$$L_i \leqslant L_{\min}. \tag{1}$$

1.1.2 Maximum yaw/pitch constraints

The maximum yaw and pitch angle constraints in UAV trajectory planning are set to ensure the stability and safety of the UAV during flight. In order to obtain a feasible trajectory, the turning range of the UAV can only be within the maximum yaw angle, and the trajectory planning in the algorithm should also satisfy the constraints of the maximum yaw angle, $\theta_{\max}$, and the maximum pitch angle, $\gamma_{\max}$[15,16].

With the UAV yaw angle/pitch angle constraints, the nodes of the extended tree in the trajectory planning need to satisfy $\theta < \theta_{\max}$ and $\gamma < \gamma_{\max}$, when X_{near}, X_{nearest}, and X_{new} are connected to form a trajectory segment that is consistent with the UAV's own flight conditions, so that the generated X_{new} can be added to the set of nodes needed. The UAV yaw angle and pitch angle constraints are show in Fig.1.

1.1.3 Maximum range constraints

The maximum range constraint in UAV trajectory planning usually refers to the fact that the navigation distance of the UAV from the takeoff point to the target point cannot exceed the preset maximum range, as long as other constraints are satisfied[6].

In the process of accomplishing the trajectory flight mission, the range of the UAV is affected by the amount of fuel or electricity on board, and the UAV trajectory flight needs to complete the flight within the maximum range $L_{\max}$. Assuming that there are j trajectory nodes during the trajectory flight, in which the trajectory range of the ith segment is L_i, the total range L of the trajectory must satisfy

$$L = \sum_{i=1}^{j-1} l_i,\ L \leqslant L_{\max}. \tag{2}$$

1.2 Cost of drone trajectory planning

The criterion for evaluating the quality of trajectory planning for quadrotor UAV is the trajectory cost, which takes into account various factors influencing the UAV's trajectory from multiple perspectives. Among them are the cost of the length of the trajectory, the cost of the threat, and the cost of the degree of smoothing. The

trajectory planning cost equation is

$$J = \omega_1 j_1 + \omega_2 j_2 + \omega_3 j_3, \tag{3}$$

where J is the total cost function of the UAV trajectory; j_1, j_2, and j_3 are the length cost, threat cost, and smoothness cost of the trajectory, respectively; ω_1, ω_2, and ω_3 are the corresponding weight coefficients. The cost of trajectory planning is shown in Fig.1.

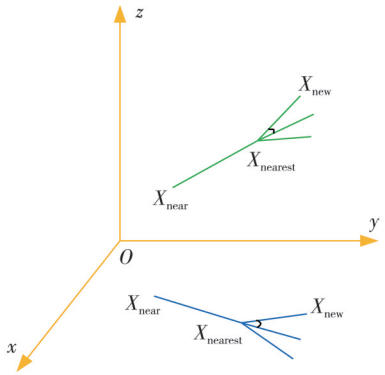

Fig. 1 UAV yaw angle/pitch angle constraints

2 Improved two-way RRT algorithm

Bidirectional RRT algorithm has largely shortened the search speed and efficiency compared with the traditional RRT algorithm, but there are still problems such as inefficiency of sampling, long search time, randomly expanding the tree may encounter many infeasible or redundant paths, and the planned trajectory is difficult to comply with the UAV constraints, etc. The bi-directional RRT algorithm will be improved from the following aspects in order to address these problems.

The bidirectional RRT algorithm is show in Fig.2.

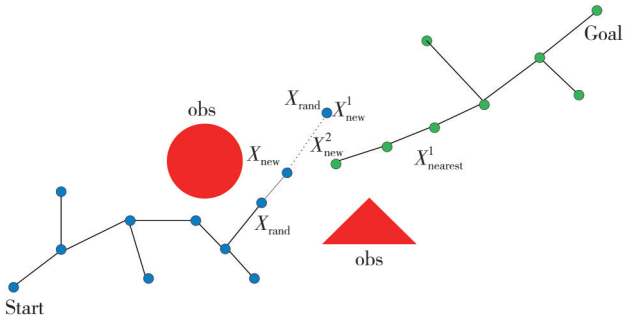

Fig. 2 Bidirectional RRT algorithm

Tree 1 and tree 2 are the starting point and end point of each other, respectively. Tree 1 obtains the sampling point X_{rand} in the space with a certain probability, searches for the nearest node $X_{nearest}$ to the node X_{rand} in the book, and checks whether the two nodes collide or not through the collision function. If there is no collision, tree 1 extends from the node $X_{nearest}$ vertically in the direction of the node X_{rand} with a step size to get a new node X_{new}, add the new node to the set, and discard it if it collides. At this time, tree 2 takes the X_{new} of tree 1 as the target point, and extends the node X^1_{new} from the nearest node $X^1_{nearest}$ to X_{new} to get node X^1_{new}, detects the collision if there is no collision and extends the node in the same way to get X^2_{new}, and extends the process to the point that it fails or when the distance to X_{new} is smaller than the set value, the two trees are directly connected. Then, all the nodes are traversed to obtain the shortest trajectory.

2.1 Goal-oriented strategy

In order to solve the problems of insufficient goal orientation and low search efficiency in the bidirectional RRT algorithm, goal orientation is applied to the bidirectional RRT algorithm. The idea of goal bias is introduced on the basis of bidirectional RRT algorithm to make it more directional. The method is to find the closest node of the starting two trees, use the idea of goal orientation to generate random points, and generate new nodes with a certain direction through the role of goal orientation, which can improve the efficiency of the search[5].

By expanding the process to add goal-oriented, this method can solve the lack of random selection of nodes and make the algorithm more efficient for the search of complex space.

$$Tree_1{:}x_{rand} = \begin{cases} x_{goal}, & P \leqslant P_{tar}, \\ SampleFree(), & P > P_{tar}, \end{cases} \tag{4}$$

$$Tree_2{:}x_{rand} = \begin{cases} x_{start}, & P \leqslant P_{tar}, \\ SampleFree(), & P > P_{tar}, \end{cases} \tag{5}$$

where P_{tar} ($P_{tar} \in [0, 1]$) is target bias probability, P ($P \in [0, 1]$) is random probability.

2.2 Artificial potential field effect

The bi-directional RRT algorithm has strong randomness at the sampling points, which leads to blind expansion of the random tree and reduces the planning speed of the algorithm. It is for this problem that the artificial potential field action is introduced.

The functions of gravitational potential field and repulsive potential field for the target point to node action in the flight environment are

$$U_{att}(n) = \frac{1}{2} k_p \cdot \rho^2(p, p_{goal}), \tag{6}$$

$$U_{rep}(n) = \begin{cases} \dfrac{1}{2} \cdot k_r \left(\dfrac{1}{\rho(p, p_{obs})} - \dfrac{1}{\rho_0} \right)^2, & \rho(p, p_{obs}) \leqslant \rho_0, \\ 0, & \rho(p, p_{obs}) > \rho_0, \end{cases} \tag{7}$$

where k_p is the size coefficient of the gravitational field, k_r is the size coefficient of the repulsive field, $\rho(p, p_{goal})$ is the

absolute value of the Euclidean distance between the point X_{near} and the target point X_{goal}, $\rho(p,p_{obs})$ is the absolute value of the Euclidean distance between the node X_{near} and the obstacle centroid, and ρ_0 is the effective radius of the distance of obstacle action.

The gravitational force is the negative gradient of the gravitational field and the repulsive force is the negative gradient of the repulsive field, which can be obtained by finding the negative gradient for the two potential field functions.

$$F_{att}(n)=-\nabla U_{att}(n)=k_p\cdot\rho(p,p_{goal}), \tag{8}$$

$$F_{rep}(n)=-\nabla U_{rep}(n)=\begin{cases}k_r\left(\dfrac{1}{\rho(p,p_{obs})}-\dfrac{1}{\rho_0}\right), & \rho(p,p_{obs})\leqslant\rho_0,\\ 0, & \rho(p,p_{obs})>\rho_0.\end{cases} \tag{9}$$

Combined force of repulsive forces of all obstacles is

$$F_{rep}=\sum_{i=1}^{n}F_{rep}(i). \tag{10}$$

The repulsive force that X_{near} can be acted upon by the obstacles obs_1 and obs_2 are $F_{rep}(1)$ and $F_{rep}(2)$, respectively, and the combined force of the two is F_{rep}, the gravitational force that X_{near} can be acted upon by the target point is F_{att}, and the combined force of the node X_{near} repulsive force, F_{rep}, and the gravitational force, F_{att}, is F. The node produced by the random tree is subjected to a combined force F, and is expanding in the direction of the combined force of the two.

The total potential field force is the vector sum of the attractive force generated by the target point and the repulsive force generated by each obstacle.

$$F=F_{att}+F_{rep}. \tag{11}$$

The bidirectional RRT in presence of an artificial is show in Fig.3.

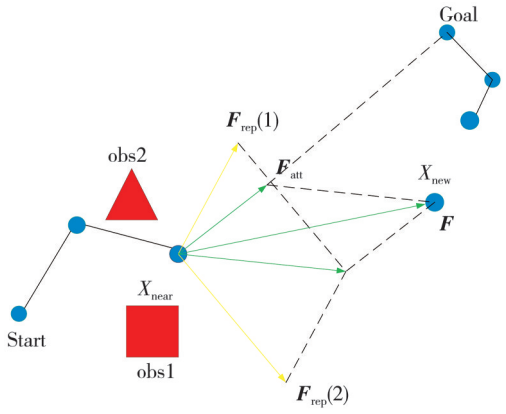

Fig. 3 Bidirectional RRT in presence of an artificial

2.3 Trigonometry

The trajectory planned by the bidirectional RRT algorithm under the effect of artificial potential field still exists with many redundant nodes, so the triangulation method is used to trim the redundant nodes[17].

The method is an idea to reduce the path length by the idea that the sum of two sides of a triangle is greater than the third side. The sequence of path nodes generated with the improved two-way RRT algorithm is $\boldsymbol{P}=[P_1, P_2,\cdots,P_i]$. When the nodes P_i and P_{i+2} are connected in a way that they are not in contact with the obstacles, then the node P_{i+1} is cropped. And after iteratively traversing through all the node sequences by using triangular delimiting method, the redundant tree nodes can be efficiently cropped, so that the length of the trajectory as well as the quality of the path can also be improved.

The triangular inequality crop is shown in Fig.4. The redundant nodes in the obstacle avoidance path are deleted by the method of taking the shortest path with two-way deletion. Firstly, the starting points Start and P_1 are linked. Then SP_2 and SP_3 are collision detected in turn. SP_3 is judged to collide with the obstacle. At this time, P_2 is retained and P_1 is deleted, and the triangulation method is effective in removing the redundant nodes in the trajectory by gradually advancing forward to traverse the target points from the starting point according to the above method. The triangulation method can effectively screen out the redundant nodes in the trajectory. This method aims to improve the search efficiency by pruning unnecessary paths in the search process.

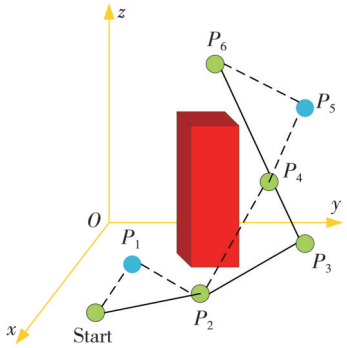

Fig. 4 Triangular inequality cut

2.4 Cubic B-spline smoothing

By pruning the redundant nodes in the obstacle avoidance path through the triangulation method, the path length can be shortened. However, there is a problem of non-smoothness at the turning points of the path. Therefore, a cubic B-spline curve is used to smooth the obstacle avoidance path.

In the space of flight, the components of the trajectory of the UAV are represented by a k-order B spline curve with $n+1$ control points, i.e.,

$$\boldsymbol{C}(u)=\sum_{i=0}^{n}\boldsymbol{N}_{i,p}(u)\boldsymbol{P}_i, \tag{12}$$

where the basis function is denoted by $N_{i,p}$(u) and the ith control point vector is denoted by $\boldsymbol{P}_i$. To compute this polynomial, the Cox -deBoor recursive formula is used.

$$\boldsymbol{N}_{i,0}(u)=\begin{cases}1, & u_i\leqslant u\leqslant u_{i+1},\\ 0, & \text{otherwise},\end{cases} \tag{13}$$

$$\boldsymbol{N}_{i,k}(u)=\frac{u-u_i}{u_{i+k}-u_i}\boldsymbol{N}_{i,k-1}(u)+\frac{u_{i+k+1}-u}{u_{i+k+1}-u_{i+1}}\boldsymbol{N}_{i+1,k-1}(u). \tag{14}$$

The parameter interval of this paper is $u\in[0,1]$. Define the node vector as $\boldsymbol{U}=[U_0,U_1\ldots U_m]$, where $u_i\leqslant u_{i+1}$, and $m=k+n+1$.

From the value of the polynomial, we can see a characteristic of the B spline curve, the whole curve is drawn without the influence of the control points, but only locally affects the direction of the curve. The B spline curve is the curve that locally controls the shape through the control points.

2.5 Algorithm flow chart

The flow chart of the improved algorithm is shown in Fig.5.

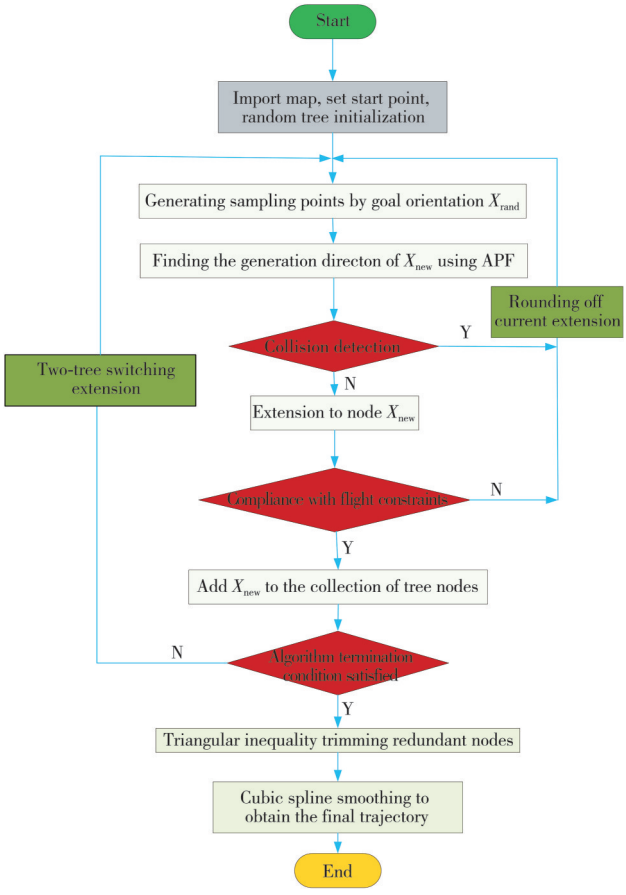

Fig. 5 Flowchart of improved bi-directional RRT algorithm

3 Simulation verification

In order to verify the superiority of the improved bidirectional RRT algorithm and to make the simulation experiments of the algorithm closer to the actual environment, we abstracted the obstacles in the actual environment into three-dimensional shapes, such as cylinders, and simplified the UAVs into mass points. However, this simplification may have led to some differences between the simulation environment and the actual trajectory environment. To be as close as possible to the actual environment, the obstacles were appropriately inflated in this study. The simulation platform used in this paper was Matlab2020a, with the operating system of the simulation environment being Windows 10, an Intel(R) Core(TM) i7-6700HQ CPU @ 2.60GHz processor, and 8 GB of running memory.

To fully illustrate the effect of the improved performance of this algorithm, the traditional RRT, bidirectional RRT algorithm, and RRT* algorithm were compared and analyzed by the simulation experiments, as well as the improved bidirectional RRT algorithm with artificial potential field action in two-dimensional and three-dimensional complex environments[18]. A comprehensive comparison was made with respect to the final path length "l" of the algorithm, the time taken to complete the trajectory search "t", and the number of nodes of the random tree expansion "n". Since the data for each trajectory planning differed, for the sake of scientific rigor, each complex environment underwent 60 experimental simulations for each of the four algorithms to increase the persuasiveness of the simulation results.

3.1 Complex square obstacles

The UAV 2D complex square obstacle environment and the simulation result is shown in Fig.6, and the simulation data is presented in Table 1. The map size is 600×600, the starting point coordinates are [10, 10], and the target point coordinates are [580, 580]. The red curve connecting the starting point and the target point represents the last trajectory searched by the algorithm, and the green curve represents the smoothed flight trajectory.

Fig. 6 shows that the RRT algorithm exhibits the highest degree of randomness in its search process, leading to variable path quality and increased instability. Additionally, Table 1 indicates that the trajectory planning time is the longest. Therefore, the improved bi-directional RRT algorithm presents overall better performance than the other three algorithms.

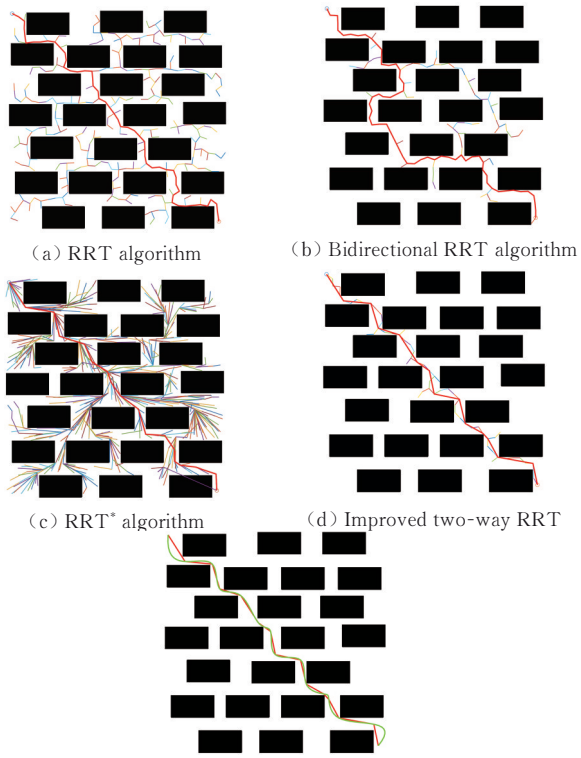

Fig. 6 Comparative simulation of algorithms in a 2D square environment

Table 1 indicates that the improved bi-directional RRT algorithm saves 11.9% and 18.7% in path length for trajectory planning compared to the RRT and bi-directional RRT algorithms.

Table 1 Mean value of each data in a two-dimensional complex square environment

Arithmetic	l/m	t/s	n
RRT	1 037.31	20.73	317
Bi-RRT	1 123.98	9.31	132
RRT*	914.32	17.44	264
Improved two-way RRT	913.23	4.61	64

Although the improved bi-directional RRT algorithm do not show a significant improvement in length compared to the RRT* algorithm, the planning time is reduced by 73.5% with the improved bi-directional RRT algorithm in comparison to the RRT* algorithm. The expansion tree nodes are reduced by 79.8%, 51.5%, and 75.7% with respect to the RRT, bi-directional RRT, and RRT* algorithms, respectively. The data analysis shows that the improved algorithm addresses the shortcomings of the RRT* regarding excessive sampling time and also resolves the issue of overly large blind searches for the traditional RRT.

3.2 Complex maze of obstacles

The two-dimensional complex maze obstacle environment of the UAV and the simulation results are shown in Fig. 7. The map size is 900×700, the coordinates of the start point are [30, 30], and the coordinates of the target point are [630, 820]. The red curve that connects the start point and the target point represents the final trajectory searched by the algorithm. The green curve is the smoothed trajectory simulation.

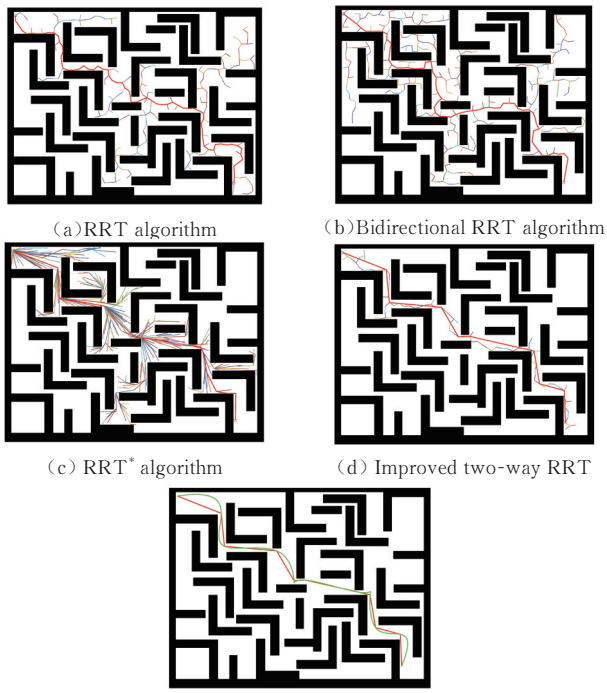

Fig. 7 Comparative simulation of algorithms in 2D maze environment

As shown in Fig. 7, the improved algorithm demonstrates its superiority even in more complex maze environments. The simulation data is presented in Table 2.

Table 2 Mean value of each data in a two-dimensional complex maze environment

Arithmetic	l/m	t/s	n
RRT	1 453.36	26.73	380
Bi-RRT	1 390.79	11.31	220
RRT*	1 253.68	25.42	344
Improved two-way RRT	1 203.57	7.02	86

It indicates that the path length is reduced by 17.1%, 13.4%, and 3.9% compared to the other three algorithms, while the trajectory elapsed time is reduced by 73.7%, 37.9%, and 72.3%. It is clear that the number of nodes still has a significant advantage.

3.3 Three-dimensional complex obstacles

The accuracy and effectiveness of the improved algorithm in the 2D complex environment were verified in the previous simulation experiments, but the UAV was not fixed at the same altitude during the real flight, and the influence of altitude on trajectory planning also needed to be

considered. The environment of the 3D simulation is 150×150×150, the coordinates of the starting point are [10,10,10], the coordinates of the target point are [150,150,50], and the cylindrical obstacles are inflated. The simulation data of the 3D environment is shown in Table 3.

A simulation comparison of the algorithm in a 3D complex environment is shown in Fig. 8. In three-dimensional space, the data in Fig.8 clearly shows that the improved two-way RRT algorithm has the best performance. The improved algorithm is influenced by the artificial potential field, which makes the random tree nodes more directional.

Table 3 Average value of each data in three-dimensional complex environments

Arithmetic	l/m	t/s	n
RRT	282.26	20.73	130
Bi-RRT	375.43	12.41	180
RRT*	271.64	9.21	70
Improved two-way RRT	270.32	4.61	62

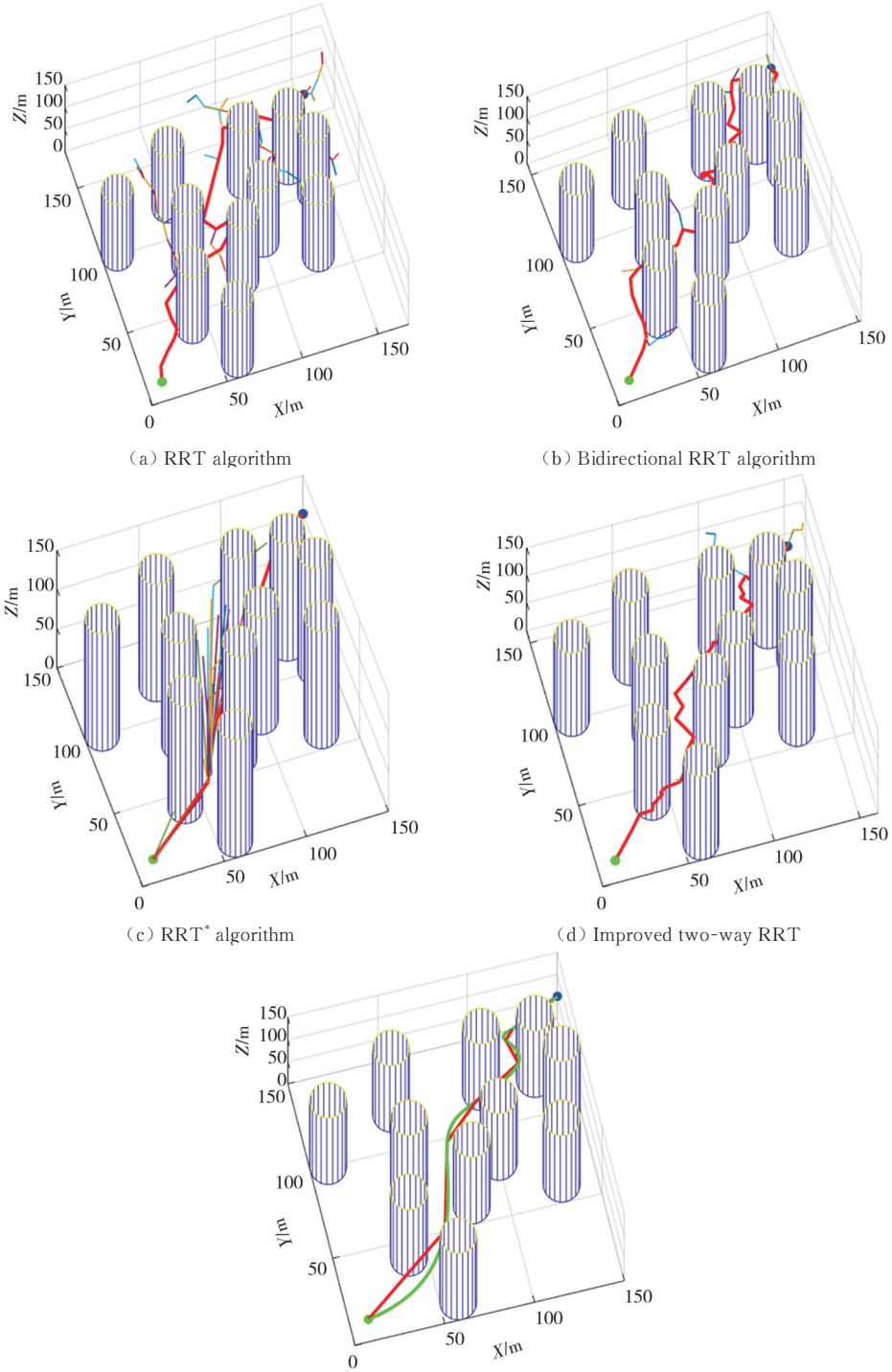

(a) RRT algorithm

(b) Bidirectional RRT algorithm

(c) RRT* algorithm

(d) Improved two-way RRT

(e) Improved algorithm after smoothing

Fig. 8 Comparative simulation of algorithms in three-dimensional complex environments

The goal-oriented approach significantly reduces the number of invalid explorations. Furthermore, taking into account the corners and other constraints of the UAV, this algorithm utilized the triangle inequality to prune redundant nodes and employed a cubic B-spline curve to perform three levels of smoothing on the trajectory. Ultimately, the planned trajectory closely matched the actual flight situation of the UAV.

Although the advantages of the improved bi-directional RRT and RRT* algorithms in the three-dimensional complex environment are not very obvious in terms of path length, the improved bi-directional RRT reduces time consumption by 49.9% compared to the RRT* algorithm. The average values of each data in the 3D complex environment are displayed in the Table 3.

Comparison of data for different environments is shown in Fig.9. It is evident that the improved two-way RRT algorithm demonstrates good performance for trajectory planning in different complex environments. The algorithm quickly planned a smooth and stable trajectory, providing a new method for solving UAV trajectory planning.

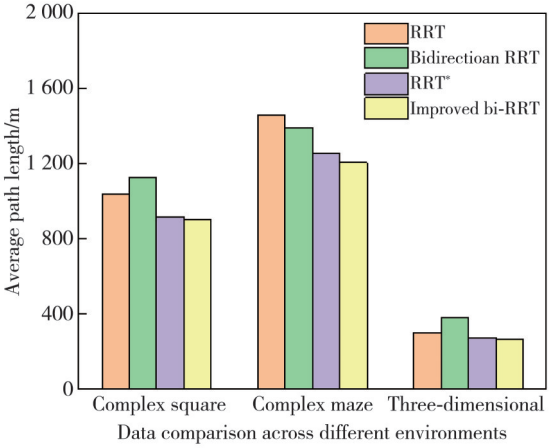

(a) Average path length comparison

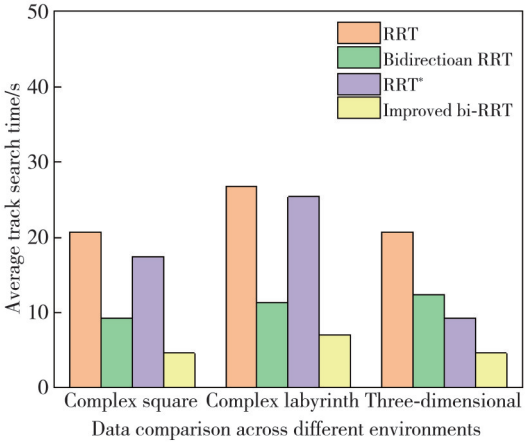

(b) Comparison of average track search time

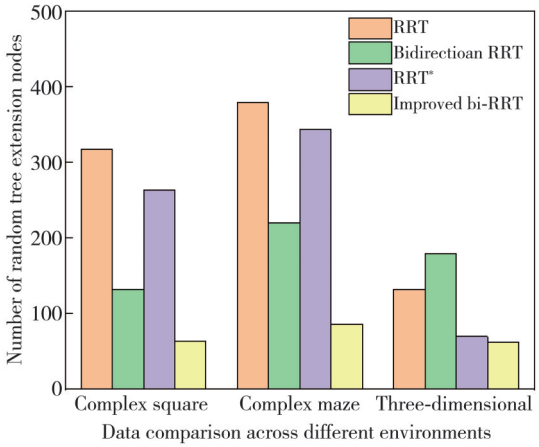

(c) Comparison of number of nodes in a random tree extension

Fig. 9 Summary of data for different environments

3.4 Online trajectory planning simulation.

Localized path planning algorithms were usually used when unknown obstacles were encountered in the working environment. The artificial potential field method, based on the concept of potential fields in physics, generated a virtual potential field around the UAV to guide its movement towards the target while ignoring obstacles. The advantage of this method was its algorithmic simplicity and the smoothness of the generated paths, but it was prone to local minima of the gradient, leading to failure in reaching the target. In this paper, the algorithm incorporated the role of the artificial potential field in the two-way RRT expansion process, which efficiently avoided obstacles and prevented falling into local minima. The following presented a comparative simulation experiment between the two-way RRT algorithm that included the artificial potential field method and the artificial potential field method itself.

A Matlab simulation experiment of dynamic path planning was performed in a three-dimensional space of $[20, 20, 20m]$ with a starting point of $[1, 1, 1m]$ and an end point of $[19, 19, 19m]$. Using the global paths after pruning and smoothing in the global path planning simulation experiments, two dynamic obstacles were created in the region to move towards the space with a certain period.

In order to further verify the performance demonstrated by the improved two-way RRT algorithm when facing dynamic obstacles, the artificial potential field method was simulated in comparison with the improved algorithm. The UAV localized path for avoiding dynamic obstacles in a 3D environment is shown in Fig.10.

The parameters in the activity range represent: obstacle's moving step in x direction, obstacle's moving step in y direction, obstacle's moving step in z direction,

obstacle's moving period (how much time to change the moving direction).

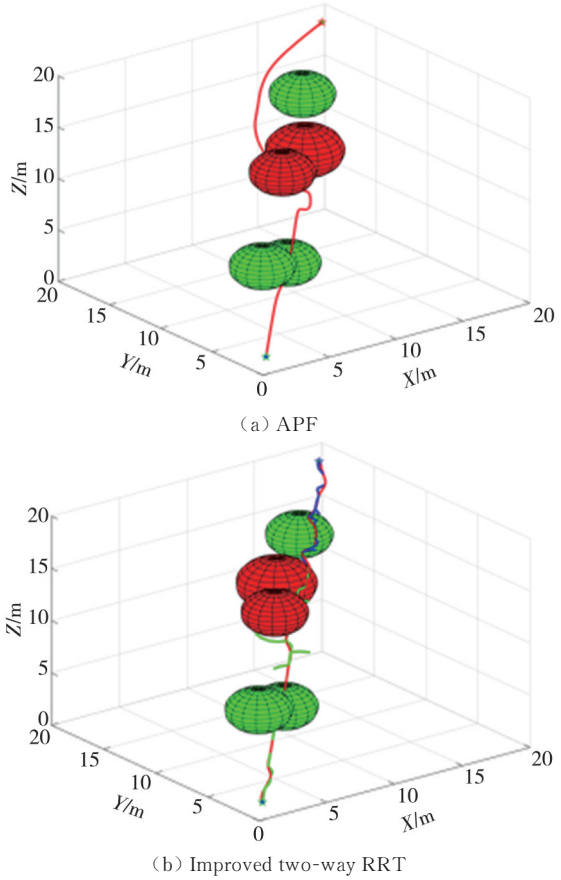

(a) APF

(b) Improved two-way RRT

Fig. 10 Comparison between artificial potential field method and improved algorithm in dynamic environments

The static and dynamic obstacle parameters are shown in Table 4.

Table 4 Static and dynamic obstacle parameters

Barrier	Color	Center coordinates	r/m	Scope of activities
Static barrier	Green	(8, 8, 4.5)	2	—
		(3.8,5,7)	2	—
		(16,17,14)	2	—
Dynamic barrier	Red	(12.5,5.7,8.6)	2	(−0.03,0.04,0.03;120)
		(15,12,10)	2.4	(−0.03,0.03,0.02;100)

The green curve and the blue curve represent the two tree extensions of the improved algorithm, while the red curve indicates the final path that avoids the dynamic obstacles. The specific data from the simulation of the two algorithms is shown in Table 5.

Table 5 Comparison of simulation data of two algorithms

Algorithm	Planning time/s	Path length/m
APF	12.23	36.23
Improved RRT	4.69	34.45

It is evident that the improved bi-directional RRT algorithm proposed in this paper quickly completes the online trajectory planning when unexpected threats arise. The data indicates that, both in terms of time and path length, the improved algorithm efficiently avoids obstacles to accomplish the task when facing dynamic obstacles.

4 Conclusions

The bidirectional RRT algorithm proposed in this paper, under the influence of artificial potential field, adopts the method of guided growth to improve the efficiency of the algorithm in space exploration and solves the problem of blind search in the bidirectional RRT algorithm. By adding a goal-oriented strategy to influence the generation of new nodes, the new nodes expand in the direction conducive to the target point, and constraints are imposed on the growth of random tree nodes, making the planned trajectory closer to the actual flight trajectory. Through triangulation, redundant nodes are effectively removed. And the problem of the zigzag trajectory is solved, making the trajectory smoother.

A large number of experimental simulation results showed that the improved algorithm in this paper had shorter path lengths than the RRT and bidirectional RRT algorithms, and could effectively shorten the planning time. Through dynamic environment experiments on this algorithm, online trajectory planning can be efficiently completed. The algorithm proposed in this paper can be extended and applied to robot arm trajectory planning and unmanned ship path planning fields. Future research will develop towards more complex dynamic and static combined path planning directions.

Acknowledgement

This work was supported by Gansu Provincial Science and Technology Program Project (No.23JRRA868); Lanzhou Municipal Talent Innovation and Entrepreneurship Project (No.2019-RC-103)

Declaration of conflicting interests

The authors have no conflict of interests related to this publication.

References

[1] CHENG J, ZHENG Y, LI C L, et al. Multi-aircraft cooperative trajectory planning algorithm for ultra-low altitude logistics scenarios. Journal of System Simulation, 2024, 36(1): 50-66.

[2] SUN F C, GAN X S. Lateral manoeuvring path planning for unmanned aerial combat confrontation between two aircraft. Modern Defence Technology, 2022, 50(3): 109-118.

[3] LIN W X, XIE W J, ZHANG P, et al. Three-dimensional path planning for unmanned aerial vehicles based on group optimization improved particle swarm algorithm. Fire Control & Command Control, 2023, 48(1): 20-25.
[4] HU H J. Intelligent trajectory planning and simulation research of rotorcraft in complex environment. Nanjing: Nanjing University of Aeronautics and Astronautics, 2023.
[5] ICHTER B, HARRISON J, PAVONE M. Learning sampling distributions for robot motion planning//2018 IEEE International Conference on Robotics and Automation, May 21-25, 2018, Brisbane, QLD, Australia. New York: IEEE, 2018: 7087-7094.
[6] DENG Y, JIANG X J. Four-rotor UAV track planning algorithm based on improved artificial potential field method. Transducer and Microsystem Technologies, 2021, 40(7): 130-133.
[7] JIANG H, CHAO Y S, ZHOU J L, et al. Improved RRT algorithm for robotic arm path planning. Machinery Design & Manufacture, 2023, 12(5): 288-292.
[8] JIANG X J, HUANG B D, YANG X J. An improved bidirectional RRTs algorithm for UAV global path planning. Mechanical Science and Technology for Aerospace Engineering, 2024, 43(5): 897-903.
[9] LIU A B, YUAN J. Robot path planning based on goal biased bidirectional RRT* algorithm. Computer Engineering and Applications, 2022, 58(6): 234-240.
[10] ZHANG S, XIE X H, CHEN D P. UAV path planning algorithm based on improved RRT-Connect. Transducer and Microsystem Technologies, 2020, 39(12): 146-148.
[11] YU C, CHEN M, YONG K N. Round-trip path planning for unmanned aerial vehicle based on improved RRT* algorithm. Scientia Sinica Technologica, 2023, 53(11): 1911-1921.
[12] HAO G Q, LV Q, HUANG Z, et al. UAV path planning based on improved artificial potential field method. Aerospace, 2023, 10(6): 562.
[13] LIAO B, WAN F Y, HUA Y, et al. F-RRT*: an improved path planning algorithm with improved initial solution and convergence rate. Expert Systems with Applications, 2021, 184: 115457.
[14] ZHANG W M, FU S X. Mobile robot path planning based on improved RRT* algorithm. Journal of Huazhong University of Science and Technology (Natural Science Edition), 2021, 49(1): 31-36.
[15] LI C L, HE J L, DENG Y, et al. Obstacle-free trajectory planning algorithm for quadrotor UAV based on improved RRT-connect. Transducer and Microsystem Technologies, 2019, 38(5): 136-139.
[16] SHIARLIS K, MESSIAS J, WHITESON S. Rapidly exploring learning trees//2017 IEEE International Conference on Robotics and Automation, May 29 - June 3, 2017, Singapore. New York: IEEE, 2017: 1541-1548.
[17] KANG J G, LIM D W, CHOI Y S, et al. Improved RRT-connect algorithm based on triangular inequality for robot path planning. Sensors, 2021, 21(2): 333.
[18] ZHANG L P, SHI X X, YI Y M, et al. Mobile robot path planning algorithm based on RRT_Connect. Electronics, 2023, 12(11): 2456.

基于改进双向RRT算法的无人机航迹规划

王梦桥，刘二林*

兰州交通大学 机电工程学院，甘肃 兰州 730070

摘　要： 针对传统RRT（Rapidly-exploring random tree）算法和双向RRT算法在复杂环境下进行无人机路径规划时存在采样效率低、采样点随机性较强和规划的路径曲折等问题，提出了改进的双向RRT算法。首先，采用目标导向策略引导采样点朝向目标点生成。然后，人工势场作用于随机树节点可以避免跟障碍物碰撞，且减少了搜索路径的长度。随机树节点生长时还结合了无人机自身飞行约束，并通过结合三角划线法去除冗余节点策略和三阶B样条曲线对航迹进行平滑处理，使得规划出的路径更优。最后，在复杂环境和动态环境中进行仿真实验。结果表明：该算法有效提高了航迹规划速度，并缩短了航迹长度，能很好的在复杂环境中生成一条安全、平滑且快速的航迹，可以应用于在线航迹规划。

关键词： 复杂环境；双向RRT算法；目标导向策略；人工势场法；三角不等式裁剪；三次B样条曲线；在线航迹规划

引用格式： WANG Mengqiao, LIU Erlin. UAV trajectory planning based on improved bidirectional RRT algorithm. Journal of Measurement Science and Instrumentation, 2025, 16(4): 578-587. DOI: 10.62756/jmsi.1674-8042.2025056